Impact of Motion And Symmetry Correction on Perfusion Lesion Segmentation in Acute Ischemic Stroke: Quantitative Evaluation

D. D. Shanbhag[1], R. Mullick[1], S. K. Nath[1], C. Oppenheim[2], M. Luby[3], K. D. Ku[3], L. L. Latour[3], S. Warach[3], and . NINDS Natural History of Stroke Investigators[3]

[1]Imaging Technologies, GE Global Research, Bangalore, Karnataka, India, [2]Department of Neuroradiology, Université Paris-Descartes, Paris, France, [3]NINDS, NIH, Bethesda, MD, United States

Introduction:

Head motion while imaging stroke is often observed during acquisition of spatio-temporal data like perfusion-weighted imaging (PWI). In stroke data analysis, retrospective motion correction is the norm due to acquisition time-constraints, while symmetry correction (SC) is used frequently for contralateral analysis. Previously it was demonstrated that the motion correction (MC) scheme along with SC provided visible improvements in the generated perfusion maps [1]. However, MC is the time-limiting step (~90% of processing time) in PWI analysis pipeline [2]. Our group has developed a fast and reliable tool for DWI and PWI lesion segmentation. In this study, we used this algorithm to address the following hypotheses: (a). Does motion correction, applied ad-hoc on all PWI datasets, provide improvements in PWI lesion segmentation? (b). Is there any difference in PWI lesion segmentation due to the order in which symmetry correction is applied: prospectively on raw PWI signal curve data or retrospectively on quantitative maps? We also introduce a method to quickly evaluate if motion is present in PWI data and suggest a strategy to apply motion correction scheme in acute stroke.

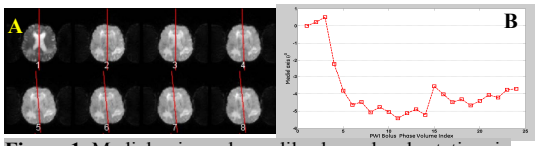

Figure 1. Medial axis angle readily shows head rotation, in terms of tilt to left, over the bolus phase volumes (fig A), which can be easily quantified and detected (fig B).

Table 2. Set #1 only.*(N = 23)*	NMC vs. GT ρ	NMC vs. GT AVD (cc)	MC vs. GT ρ	MC vs. GT AVD (cc)
MTT based PWI lesion Seg	0.91	44±33	0.9	43±39

Methods and Materials ***Patient database:*** Data for our study was acquired from 2000 through 2008, from patients treated with standard IV-tPA after a baseline, pre-treatment MRI at multiple centers. The appropriate IRBs approved the studies. We segregated our database into two datasets, one for which the ground-truth (GT): DWI and PWI lesion markings were available (Set#1, N = 23) and other for which no GT was done (Set#2, N= 68). ***Imaging:*** All the datasets were obtained on a 1.5T GE Signa Genesis and GE Signa HDx clinical scanners using an 8-channel head or NV coil. (a). DWI imaging: Axial DWI trace images were acquired using a SE-EPI sequence, TE = 67 ms – 100 ms, TR = 4.5s – 7s, FA = 90°, NEX = 2, matrix = 256 x 256, FOV = 240x 240 mm^2, slice thickness varying from 3.5mm to 7 mm, b = 0 s/mm^2 and 1000 s/mm^2. (b) PWI Imaging: Axial oblique slices were acquired using a GE-EPI sequence, TE = 19 ms – 60 ms, TR = 1s – 2.275s, FA = 90°, number of phases from: 25 (2 s/phase) to 100 (1s/phase), slice thickness = 5 mm – 7mm, matrix size = 64 x 64 -128 x 128, FOV = 240x 240 mm^2. ***PWI Map generation:*** The mismatch calculator tool-calculated maps used for PWI lesion segmentation, with the current study using first moment MTT and Tmax maps for analysis [3]. ***Image Analysis:*** *(a). PWI segmentation:* PWI segmentation is based on contra-lateral difference analysis of SC, skull stripped quantitative maps, along with feedback from the co-registered DWI and ADC maps. For each map, an optimal difference threshold (Δ) was calculated using regional statistics for contra-lateral analysis. A clustering algorithm collated the disjoint islands from contra lateral analysis into single ensemble lesion and rejected noise islands. The final perfusion lesion was obtained by removing the ventricles from the clustered lesion mask, and generic hole filling. ***Motion Schemes:*** Details about motion scheme/SC have been described elsewhere [1] and only important steps are described here. **StepP1.** Reformat temporal raw signal data into multi-phase 3D volumes; **StepP2.** Apply a SC step, using nearest neighborhood interpolation. *No Motion Correction (NMC) scheme*: StepP1 → StepP2 → PWI Map → PWI Seg was implemented. *MC scheme:* StepP1 → StepP2, followed by {(a). Gradient descent optimization of multiple rigid transforms (affine and quaternion) with respect to a Mutual Information metric with the reference image (t=TR) and all phases thereafter; (b). Tri-linear interpolation of PWI bolus- phase volumes based on the optimum transform} → PWI Map → PWI Seg was implemented. Data from both Set#1 and Set#2 were used. ***SC ordering scheme:*** A subset from Set#1 (N =13) and Set #2 (N = 9), which did not show any significant motion, were selected to demonstrate the effect of SC ordering on PWI lesion segmentation. For **SC-Pros** ordering, StepP1 → StepP2 → PWI Map → PWI Seg was implemented. For **SC-Post** ordering, StepP1 → PWI Map → StepP2 {map only} → PWI Seg was implemented. The entire pipeline (MC, NMC, SC, registration, map generation and lesion segmentation) was implemented using the functionality available in the Insight Toolkit (ITK) [4]. *(b) GT generation and evaluation:* A trained imaging scientist marked lesion locations on DWI images and MTT maps, smoothened and interpolated to match DWI matrix size, which formed the ground truth [5]. *(c) Motion Detection:* Image moments based approach was used to estimate motion across the bolus contrast phases in PWI data. Brain masks were generated for 3 largest slices in brain data, for each phase volume. Motion was quantified in terms of medial axis rotation angle and major axis/minor axis length determined from brain mask slices. The motion affected phase volume was identified as the one that shows deviation in any or combination of these metrics, after accounting for variations due changing nature of the bolus signal curve. Currently we report the deviant phases to the user and plan to the integrate it in the PWI analysis pipeline. ***Statistical analysis:*** *(a) Motion scheme:* **Set#1 only:** For both NMC and MC schemes, MTT map based PWI lesion segmentation was compared to GT by determining: A. Spearman correlation (ρ). B. Absolute volume differences (AVD). **Pooled Data:** Next we pooled the perfusion lesion segmentation volumes from both Set#1 and Set#2, separately for MTT based and Tmax based lesion segmentation. Repeated measures ANOVA was used on the pooled data to determine any differences between the perfusion lesion segmentation between the two motion schemes (NMC and MC). This evaluation was done separately for MTT-based and Tmax based lesion segmentation. *(b) Symmetry correction ordering scheme:* Data from two ordering schemes were tested to determine the difference between their means using repeated measures ANOVA. Testing was done separately for MTT and T_{max} based results. Statistical analyses were performed with MedCalc®(v. 10.4) software.

Table 1.	MTT based PWI lesion (cc)	
Set #1 Only *(N = 23)*	[Mean±SD]	IQR
GT	188±131	83-247
NMC	175±126	73-284
MC	174±119	76-260

Table 3 *(N =22)* * *(p < 0.01)*	MTT based PWI lesion (cc)	T_{max} based PWI lesion (cc)	MTT Δ (s)	T_{max} Δ (s)
SC-Pros	221±25	199±20	2.28±0.18	3.6±0.25
SC-Post	191±24	180±20	2.55±0.14	3.0±0.24
Difference	30±10*	19±8*	0.27 ±0.07*	0.6±0.2*

Table 3. PWI lesion segmentation result for SC ordering scheme. Data consisted of subsets from Set#1 (N =13) and Set#2 (N=9)

Results and Discussion: *Motion Scheme:* MTT based PWI lesion volumes obtained from NMC and MC showed similar correlations and absolute volume differences, compared to GT (Tables 1 and 2). Repeated measures ANOVA of pooled data did not show any statistically significant differences between the NMC and MC PWI lesion volumes, obtained from their respective MTT and T_{max} maps. *SC order scheme:* For both MTT and T_{max} based lesion segmentation, it was observed that the lesion volume with SC-Pros ordering was significantly elevated compared to SC-Post ordering (Table 3). A further investigation revealed that the difference arose due to lower threshold determined by the algorithm for SC-Pros ordering, compared to SC-Post ordering (Table 3). For a fixed threshold difference, e.g. 6s with Tmax, this effect may be insignificant; it may however impact segmentation algorithms which use image based metric to evaluate thresholds. For 13 datasets from Set#1 in which GT was available, the GT PWI lesion volume (213±129 cc) compared well to MTT based SC-Pros segmented lesion volume (221±115 cc) than MTT based SC-Post (149±112 cc) segmented lesion volume. Currently we used a nearest neighborhood approximation for SC correction. It would be interesting to ascertain this effect with different interpolation scheme(s), such a trilinear interpolation used for motion correction. Figure 1 shows the output of the moments based motion detection on a case with visible patient head motion. Fig.1B clearly shows the head motion and suggests that a time-optimal motion correction scheme would be to register the first five volumes to the sixth stable volume.

Conclusions: Applying motion correction on non-motion affected PWI datasets does not produce any significant change in segmented lesion volumes, and should be selectively applied when significant motion is detected. Symmetry correction ordering can potentially change map dynamics and from a contra-lateral analysis standpoint should be used preferably on the PWI signal volumes, rather than retrospectively on generated maps. An image moments-based scheme can readily help identify phases requiring motion correction and reduce the analysis time in an acute stroke setting.

References: [1] ISMRM Proc. 2009; Vol. 17, pg. 4710. [2]. ISMRM Proc.2009; Vol. 17, pg. 728. [3]. MRM 2003; 50:164-174 [4]. http://www.itk.org. [5] AJNR 28:1674-78, 2007.